
Learning Proposals for Practical Energy-Based Regression

Fredrik K. Gustafsson
Dept. of Information Technology
Uppsala University, Sweden

Martin Danelljan
Computer Vision Lab
ETH Zürich, Switzerland

Thomas B. Schön
Dept. of Information Technology
Uppsala University, Sweden

Abstract

Energy-based models (EBMs) have experienced a resurgence within machine learning in recent years, including as a promising alternative for probabilistic regression. However, energy-based regression requires a proposal distribution to be manually designed for training, and an initial estimate has to be provided at test-time. We address both of these issues by introducing a conceptually simple method to automatically learn an effective proposal distribution, which is parameterized by a separate network head. To this end, we derive a surprising result, leading to a unified training objective that jointly minimizes the KL divergence from the proposal to the EBM, and the negative log-likelihood of the EBM. At test-time, we can then employ importance sampling with the trained proposal to efficiently evaluate the learned EBM and produce stand-alone predictions. Furthermore, we utilize our derived training objective to learn mixture density networks (MDNs) with a jointly trained energy-based teacher, consistently outperforming conventional MDN training on four real-world regression tasks within computer vision. Code is available at https://github.com/fregu856/ebms_proposals.

1 INTRODUCTION

Energy-based models (EBMs) (LeCun et al., 2006) have been extensively studied within the field of machine learning in the past (Teh et al., 2003; Bengio et al., 2003; Mnih and Hinton, 2005; Hinton et al., 2006; Osadchy et al., 2005). By using deep neural networks to parameterize the energy function (Xie et al., 2016), EBMs

have recently also experienced a significant resurgence. Most widely, EBMs are now employed for generative modelling tasks (Xie et al., 2017; Gao et al., 2018; Xie et al., 2018c; Nijkamp et al., 2019; Du and Mordatch, 2019; Grathwohl et al., 2020; Gao et al., 2020; Pang et al., 2020; Bao et al., 2020; Du et al., 2021). Recent work has further demonstrated the promise of EBMs for probabilistic regression, achieving impressive results for a variety of important low-dimensional regression tasks, including object detection, visual tracking, pose estimation, age estimation and robot policy learning (Danelljan et al., 2020; Gustafsson et al., 2020a,b, 2021; Hendriks et al., 2021; Murphy et al., 2021; Florence et al., 2021).

Probabilistic regression aims to estimate the predictive conditional distribution $p(y|x)$ of the target y given the input x (Kendall and Gal, 2017; Lakshminarayanan et al., 2017; Chua et al., 2018; Gast and Roth, 2018; Ilg et al., 2018; Makansi et al., 2019; Varamesh and Tuytelaars, 2020). As its primary advantage, the EBM directly represents this distribution by a neural network through a learnable energy function $f_{\theta}(x, y)$, as $p(y|x; \theta) = e^{f_{\theta}(x, y)} / Z(x, \theta)$. While this flexibility allows the EBM to learn highly complex and accurate distributions, it comes at a significant cost. Firstly, evaluating the resulting distribution $p(y|x; \theta)$ is generally intractable, as it requires the computation of the partition function $Z(x, \theta)$. This particularly imposes challenges for training the EBM, which often leads to application of Monte Carlo approximations with hand-tuned proposal distributions in order to pursue maximum likelihood-based learning. Secondly, EBMs are known to be difficult to sample from, which complicates their practical use at test-time. To produce predictions, prior work (Danelljan et al., 2020; Gustafsson et al., 2020a,b, 2021) resort to gradient-based refinement of an initial estimate generated by a separately trained network.

In this work, we address both aforementioned drawbacks of this energy-based regression approach by jointly learning a proposal distribution q during EBM training. Specifically, we parametrize the proposal us-

Proceedings of the 25th International Conference on Artificial Intelligence and Statistics (AISTATS) 2022, Valencia, Spain. PMLR: Volume 151. Copyright 2022 by the author(s).

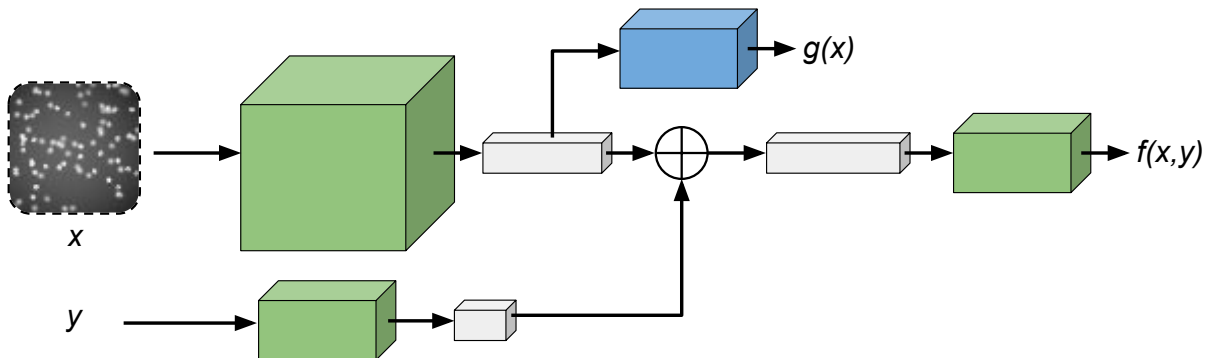


Figure 1: We propose a method to automatically learn an effective MDN proposal $q(y|x; \phi)$ (blue) during training of the EBM $p(y|x; \theta)$ (green), thus addressing the main practical limitations of energy-based regression. The MDN q is trained by minimizing its KL divergence to the EBM p , i.e. by minimizing $D_{\text{KL}}(p \parallel q)$.

ing a mixture density network (MDN) (Bishop, 1994) $q(y|x; \phi)$ conditioned on the input x . In order to maximize its effectiveness during training, we learn q by minimizing its Kullback–Leibler (KL) divergence to the EBM p . To this end, we derive a surprising result, consisting of a unified objective that jointly minimizes the KL divergence from the proposal q to the EBM p and the negative log-likelihood (NLL) of the latter. As our result does not rely on the reparameterization trick, it is directly applicable to a wide class of proposal distributions, including mixture models. Compared to previous approaches for training EBMs for regression, our approach does not require tedious hand-tuning of the proposal distribution, instead providing a fully learnable alternative. Moreover, rather than conditioning on the ground-truth target y , our proposal distribution q is conditioned on the input x . It can therefore be employed at test-time to efficiently evaluate and sample from the EBM.

Learning the MDN q according to our derived objective leads to another interesting observation: MDNs trained to mimic the EBM via this objective tend to learn more accurate predictive distributions compared to an MDN trained with the standard NLL loss. Inspired by this finding, we apply our derived result for a second purpose, namely to find a better learning formulation for MDNs. When jointly trained with an energy-based teacher network according to our objective, the resulting MDN is shown to consistently outperform the NLL baseline on challenging real-world regression tasks. In contrast to a single ground-truth sample, the EBM provides comprehensive supervision for the predictive distribution q , leading to a more accurate model of the underlying true distribution.

In summary, our main contributions are as follows:

- We derive an efficient and convenient objective that can be employed to train a parameterized distribution $q(y|x; \phi)$ by directly minimizing its KL diver-

gence to a conditional EBM.

- We employ the proposed objective to jointly learn an effective MDN proposal distribution during EBM training, thus addressing the main practical limitations of energy-based regression.
- We further utilize the proposed objective to improve training of stand-alone MDNs, learning more accurate predictive distributions compared to MDNs trained by minimizing the NLL.
- We perform comprehensive experiments on four challenging computer vision regression tasks.

2 BACKGROUND

Regression entails learning to predict targets $y^* \in \mathcal{Y}$ from inputs $x^* \in \mathcal{X}$, given a training set of N i.i.d. input-target pairs $\{(x_i, y_i)\}_{i=1}^N$, $(x_i, y_i) \sim p(x, y)$. The target space \mathcal{Y} is continuous, $\mathcal{Y} = \mathbb{R}^K$ for some $K \geq 1$. We focus on probabilistic regression, which aims to not only produce a prediction y^* , but also estimate the full predictive conditional distribution $p(y|x)$. This probabilistic formulation provides a more general view of the regression problem, allowing for the encapsulation of uncertainty, generation of multiple hypotheses, and handling of ill-posed settings (Kendall and Gal, 2017; Lakshminarayanan et al., 2017; Chua et al., 2018; Gast and Roth, 2018; Ilg et al., 2018; Makansi et al., 2019; Varamesh and Tuytelaars, 2020).

2.1 Energy-Based Regression

In energy-based regression (Danelljan et al., 2020; Gustafsson et al., 2020a,b), the task is addressed by learning to model the distribution $p(y|x)$ with a conditional EBM $p(y|x; \theta)$, defined according to,

$$p(y|x; \theta) = \frac{e^{f_\theta(x,y)}}{Z(x, \theta)}, \quad Z(x, \theta) = \int e^{f_\theta(x,\tilde{y})} d\tilde{y}. \quad (1)$$

The EBM $p(y|x; \theta)$ is directly specified via $f_\theta : \mathcal{X} \times \mathcal{Y} \rightarrow \mathbb{R}$, a deep neural network (DNN) mapping any input-target pair $(x, y) \in \mathcal{X} \times \mathcal{Y}$ to a scalar $f_\theta(x, y) \in \mathbb{R}$. The EBM in (1) is therefore highly flexible and capable of learning complex distributions directly from data. However, the resulting distribution $p(y|x; \theta)$ is also challenging to evaluate or sample from, since its partition function $Z(x, \theta)$ generally is intractable. The EBM $p(y|x; \theta)$ is therefore quite challenging to train, and a variety of different approaches have recently been explored (Gustafsson et al., 2020b; Song and Kingma, 2021). The most straightforward approach would be to directly minimize the NLL $\mathcal{L}(\theta) = \sum_{i=1}^N \log Z(x_i, \theta) - f_\theta(x_i, y_i)$. While exact computation of $\mathcal{L}(\theta)$ is intractable, importance sampling can be utilized to approximate the $\log Z(x_i, \theta)$ term. The DNN $f_\theta(x, y)$ can therefore be trained by minimizing the resulting loss,

$$J(\theta) = \frac{1}{N} \sum_{i=1}^N \log \left(\frac{1}{M} \sum_{m=1}^M \frac{e^{f_\theta(x_i, y_i^{(m)})}}{q(y_i^{(m)})} \right) - f_\theta(x_i, y_i), \quad (2)$$

where $\{y_i^{(m)}\}_{m=1}^M \sim q(y)$ are M samples drawn from a proposal distribution $q(y)$. The aforementioned approach is relatively simple, yet it has been shown effective for various regression tasks within computer vision (Danelljan et al., 2020; Gustafsson et al., 2020a,b). In these works, the proposal $q(y)$ is set to a mixture of K Gaussian components centered at the true target y_i , i.e. $q(y) = \frac{1}{K} \sum_{k=1}^K \mathcal{N}(y; y_i, \sigma_k^2 I)$. Training thus requires the task-dependent hyperparameters K and $\{\sigma_k^2\}_{k=1}^K$ to be carefully tuned, limiting general applicability. Moreover, this proposal $q(y)$ depends on y_i and can therefore only be utilized during training. To produce a prediction y^* at test-time, previous energy-based regression methods (Danelljan et al., 2020; Gustafsson et al., 2020a,b, 2021; Hendriks et al., 2021; Murphy et al., 2021) employ gradient ascent to refine an initial estimate \hat{y} . This prediction strategy therefore requires access to a good initial estimate. Hence, most previous works (Danelljan et al., 2020; Gustafsson et al., 2020a,b, 2021) even rely on a separately trained DNN to provide \hat{y} , further limiting general applicability.

2.2 Mixture Density Networks

Alternatively, the regression task can be addressed by learning to model the conditional distribution $p(y|x)$ with an MDN $q(y|x; \phi)$ (Bishop, 1994; Makansi et al., 2019; Li and Lee, 2019; Varamesh and Tuytelaars, 2020). An MDN is a mixture of K components of a certain base distribution. Specifically for a Gaussian MDN, the distribution $q(y|x; \phi)$ is defined according to,

$$q(y|x; \phi) = \sum_{k=1}^K \pi_\phi^{(k)}(x) \mathcal{N}(y; \mu_\phi^{(k)}(x), \sigma_\phi^{(k)}(x)I), \quad (3)$$

where the set of Gaussian mixture parameters $\{\pi_\phi^{(k)}, \mu_\phi^{(k)}, \sigma_\phi^{(k)}\}_{k=1}^K$ is outputted by a DNN $g_\phi(x)$. In contrast to EBMs, the MDN distribution $q(y|x; \phi)$ is by design simple to both evaluate and sample from. The DNN $g_\phi(x)$ can thus be trained by directly minimizing the NLL $\mathcal{L}(\phi) = \sum_{i=1}^N -\log q(y_i|x_i; \phi)$. While MDNs generally are less flexible models than EBMs, they are still capable of capturing multi-modality and other more complex features of the true distribution $p(y|x)$. MDNs thus offer a convenient yet quite flexible alternative to EBMs. Training an MDN $q(y|x; \phi)$ via the NLL is however known to occasionally suffer from certain inefficiencies such as mode-collapse, and various more sophisticated training methods have therefore been explored (Hjorth and Nabney, 1999; Rupprecht et al., 2017; Makansi et al., 2019; Cui et al., 2019; Zhou et al., 2020).

3 METHOD

We first address the main practical limitations of energy-based regression by proposing a method to automatically learn an effective proposal $q(y; \phi)$ during training of the EBM $p(y|x; \theta)$ in (1). To enable $q(y; \phi)$ to be utilized also at test-time, we condition it on the input x instead of on the true target y_i . We further require the resulting proposal distribution $q(y|x; \phi)$ to be flexible, yet efficient and convenient to evaluate and sample from. In this work, we therefore parametrize the proposal $q(y|x; \phi)$ using an MDN.

When training the EBM $p(y|x; \theta)$ by minimizing the approximated NLL in (2), we wish to use the proposal $q(y|x; \phi)$ that yields the best possible NLL approximation. In general, this is achieved when the proposal equals the EBM, i.e. when $q(y|x; \phi) = p(y|x; \theta)$ ¹. We therefore aim to learn the proposal parameters ϕ by directly minimizing the KL divergence to the EBM, $D_{\text{KL}}(p \parallel q)$. While this approach is conceptually simple and attractive, exact computation of $D_{\text{KL}}(p \parallel q)$ is intractable. This calls for an effective and efficient approximation, which can easily be employed during training. In Section 3.1 we show that such an approximation, interestingly enough, is achieved by simply minimizing the objective (2) w.r.t. the proposal $q(y|x; \phi)$.

In Section 3.2, we further employ this result to design a method for jointly learning the EBM $p(y|x; \theta)$ and MDN proposal $q(y|x; \phi)$. There, we also detail how $q(y|x; \phi)$ can be utilized with importance sampling to approximately evaluate and sample from the EBM at test-time. Lastly, in Section 3.3 we propose to utilize our derived approximation of $D_{\text{KL}}(p \parallel q)$ as an addi-

¹Details are provided in the supplementary material.

tional loss for training MDNs. We argue that guiding an MDN towards a more flexible and accurate distribution learned by the EBM provides more extensive supervision for the MDN in a regression setting, leading to improved results.

3.1 Learning the Proposal to Match an EBM

We have a parameterized distribution $q(y|x; \phi)$ that we want to be a close approximation of the EBM $p(y|x; \theta)$. Specifically, we want to find the parameters ϕ that minimize the KL divergence between $q(y|x; \phi)$ and the EBM $p(y|x; \theta)$. Therefore, we seek to compute $\nabla_{\phi} D_{\text{KL}}(p(y|x; \theta) \parallel q(y|x; \phi))$, i.e. the gradient of the KL divergence w.r.t. ϕ . The gradient $\nabla_{\phi} D_{\text{KL}}$ is generally intractable, but can be conveniently approximated by the following result.

Result 1 For a conditional EBM $p(y|x; \theta) = e^{f_{\theta}(x,y)} / \int e^{f_{\theta}(x,\tilde{y})} d\tilde{y}$ and distribution $q(y|x; \phi)$,

$$\nabla_{\phi} D_{\text{KL}}(p \parallel q) \approx \nabla_{\phi} \log \left(\frac{1}{M} \sum_{m=1}^M \frac{e^{f_{\theta}(x, y^{(m)})}}{q(y^{(m)}|x; \phi)} \right), \quad (4)$$

where $\{y^{(m)}\}_{m=1}^M$ are M independent samples drawn from $q(y|x; \phi)$.

A complete derivation of Result 1 is provided in the supplementary material. Note that the samples $\{y^{(m)}\}_{m=1}^M$ in (4) are drawn from $q(y|x; \phi)$ but *not* considered functions of ϕ , making this approximation particularly simple to compute in practice. Importantly, the approximation (4) does *not* rely on the reparameterization trick and is therefore directly applicable for a wide class of distributions $q(y|x; \phi)$, including mixture models. Given data $\{x_i\}_{i=1}^N$, Result 1 implies that $q(y|x; \phi)$ can be trained to approximate the EBM $p(y|x; \theta)$ by minimizing the loss,

$$J_{\text{KL}}(\phi) = \frac{1}{N} \sum_{i=1}^N \log \left(\frac{1}{M} \sum_{m=1}^M \frac{e^{f_{\theta}(x_i, y_i^{(m)})}}{q(y_i^{(m)}|x_i; \phi)} \right), \quad (5)$$

where $\{y_i^{(m)}\}_{m=1}^M \sim q(y|x_i; \phi)$. Note that $J_{\text{KL}}(\phi)$ is identical to the first term of the EBM loss $J(\theta)$ in (2). In fact, since the second term $f_{\theta}(x_i, y_i)$ in (2) does not depend on ϕ , (2) can be used as a joint objective for training both $q(y|x; \phi)$ and the EBM $p(y|x; \theta)$.

3.2 Practical Energy-Based Regression

We first employ Result 1 to jointly train the EBM $p(y|x; \theta) = e^{f_{\theta}(x,y)} / \int e^{f_{\theta}(x,\tilde{y})} d\tilde{y}$ and the MDN proposal $q(y|x; \phi)$. We define the MDN $q(y|x; \phi)$ by adding a second network head g_{ϕ} onto the same backbone feature extractor shared with the EBM DNN f_{θ} . The MDN head g_{ϕ} outputs the Gaussian mixture model

parameters $\{\pi_{\phi}^{(k)}, \mu_{\phi}^{(k)}, \sigma_{\phi}^{(k)}\}_{k=1}^K$, as defined in (3). The resulting overall network architecture is illustrated in Figure 1.

3.2.1 Training

We train the EBM $p(y|x; \theta)$ and MDN proposal $q(y|x; \phi)$ jointly using standard techniques based on stochastic gradient descent. At each iteration, we first predict the MDN mixture parameters $\{\pi_{\phi}^{(k)}, \mu_{\phi}^{(k)}, \sigma_{\phi}^{(k)}\}_{k=1}^K$ and draw M samples $\{y_i^{(m)}\}_{m=1}^M \sim q(y|x_i; \phi)$ from the resulting distribution. The MDN parameters ϕ are then updated via $J_{\text{KL}}(\phi)$ in (5), while the EBM parameters θ are updated via $J(\theta)$ in (2). In fact, this can be implemented by jointly minimizing (2) w.r.t. both θ and ϕ .

EBMs can however be trained also via various alternative approaches, including noise contrastive estimation (NCE) (Gutmann and Hyvärinen, 2010; Ma and Collins, 2018). How EBMs should be trained specifically for regression tasks was extensively studied in (Gustafsson et al., 2020b), concluding that NCE should be considered the go-to method. NCE entails training the EBM DNN f_{θ} by minimizing the loss,

$$J_{\text{NCE}}(\theta) = -\frac{1}{N} \sum_{i=1}^N J_{\text{NCE}}^{(i)}(\theta),$$

$$J_{\text{NCE}}^{(i)}(\theta) = \log \frac{\exp\{f_{\theta}(x_i, y_i^{(0)}) - \log q(y_i^{(0)})\}}{\sum_{m=0}^M \exp\{f_{\theta}(x_i, y_i^{(m)}) - \log q(y_i^{(m)})\}}, \quad (6)$$

where $y_i^{(0)} \triangleq y_i$, and $\{y_i^{(m)}\}_{m=1}^M$ are M samples drawn from a noise distribution $q(y)$. The NCE loss $J_{\text{NCE}}(\theta)$ in (6) can be interpreted as the softmax cross-entropy loss for a classification problem, distinguishing the true target y_i from the M noise samples $\{y_i^{(m)}\}_{m=1}^M \sim q(y)$. Moreover, $J_{\text{NCE}}(\theta)$ has much similarity with the importance sampling-based loss $J(\theta)$ in (2) (Ma and Collins, 2018; Jozefowicz et al., 2016). In particular, the noise distribution $q(y)$ in NCE directly corresponds to the the proposal q in (2). In fact, all prior work (Gustafsson et al., 2020b, 2021; Hendriks et al., 2021) on energy-based regression using NCE has employed the same manually designed distribution $q(y) = \frac{1}{K} \sum_{k=1}^K \mathcal{N}(y; y_i, \sigma_k^2 I)$. Due to the close relationship between NCE and importance sampling, our approach for learning the proposal distribution q is also applicable for NCE-based training of the EBM. In this work, we therefore adopt the NCE loss to train the EBM $p(y|x; \theta)$, since it has been shown to achieve favorable results (Gustafsson et al., 2020b).

Our approach still entails jointly training the EBM $p(y|x; \theta)$ and MDN $q(y|x; \phi)$, but employs NCE with

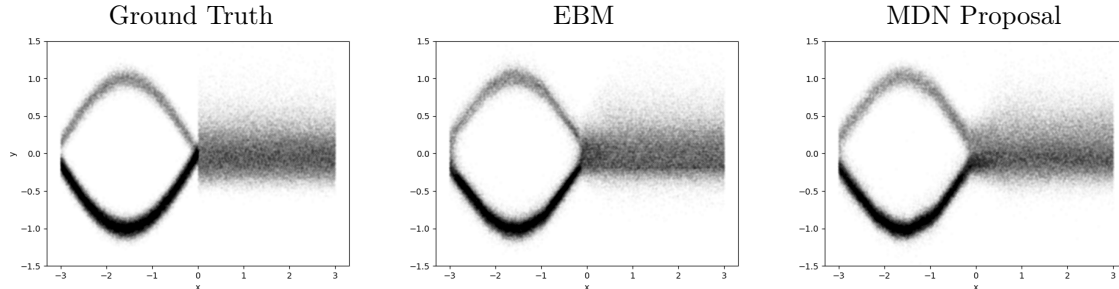


Figure 2: An illustrative 1D regression problem (Gustafsson et al., 2020b), demonstrating the effectiveness of our proposed method to jointly train an EBM $p(y|x; \theta)$ and MDN proposal $q(y|x; \phi)$. In this example, the MDN has $K = 4$ components. The EBM is trained using NCE with $q(y|x; \phi)$ acting as the noise distribution, whereas the MDN is trained by minimizing its KL divergence to $p(y|x; \theta)$, i.e. by minimizing $D_{\text{KL}}(p \parallel q)$.

$q(y|x; \phi)$ acting as a noise distribution for training the EBM. At each iteration we thus draw samples $\{y_i^{(m)}\}_{m=1}^M \sim q(y|x_i; \phi)$, update ϕ via the loss $J_{\text{KL}}(\phi)$ in (5), and update θ via $J_{\text{NCE}}(\theta)$ in (6). Note that the update of the MDN parameters ϕ only affects the added network head in Figure 1, not the feature extractor. The effectiveness of this proposed joint training method is demonstrated on an illustrative 1D regression problem in Figure 2. In the supplementary material (Figure S3), we also show an example of how both the EBM and the MDN proposal iteratively converge towards the ground truth during joint training.

Training an EBM using our joint training method is somewhat slower than using standard NCE with the manually designed $q(y) = \frac{1}{K} \sum_{k=1}^K \mathcal{N}(y; y_k, \sigma_k^2 I)$, since we now also have to update the added network head g_ϕ of the MDN proposal at each iteration. For both methods, the main computational bottleneck is however the backbone feature extractor. In fact, our proposed method usually requires less total training in practice, since the task-dependent hyperparameters K and $\{\sigma_k^2\}_{k=1}^K$ have to be tuned for the NCE baseline.

3.2.2 Prediction

To avoid evaluating the intractable $Z(x^*, \theta)$ at test-time, previous work on energy-based regression (Danelljan et al., 2020; Gustafsson et al., 2020a,b, 2021) approximately compute $\arg \max_y p(y|x^*; \theta) = \arg \max_y f_\theta(x^*, y)$ to produce a prediction y^* . Specifically, T steps of gradient ascent, $y \leftarrow y + \lambda \nabla_y f_\theta(x^*, y)$, is used to refine an initial estimate \hat{y} , moving it towards a local maximum of $f_\theta(x^*, y)$. While shown to produce highly accurate predictions, this approach requires a good initial estimate \hat{y} to be provided at test-time, limiting its general applicability.

In contrast to previous work (Danelljan et al., 2020; Gustafsson et al., 2020a,b, 2021), we have access to a proposal $q(y|x; \phi)$ that is conditioned only on the

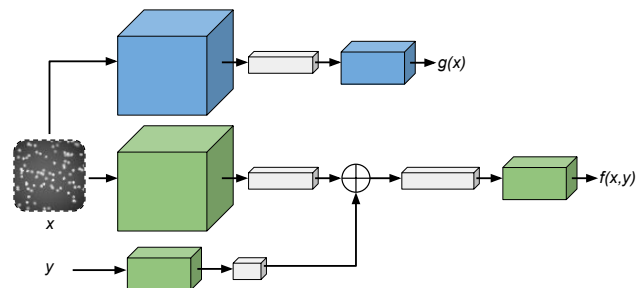


Figure 3: We extend our method of jointly training an EBM $p(y|x; \theta)$ (green) and MDN $q(y|x; \phi)$ (blue), improving MDN training. Instead of defining the MDN by adding a network head onto the EBM (Figure 1), the MDN is now defined in terms of a full DNN g_ϕ .

input x and thus can be utilized also at test-time. Since our MDN proposal $q(y|x; \phi)$ has been trained to approximate the EBM $p(y|x; \theta)$, it can be utilized with self-normalized importance sampling (Owen, 2013) to efficiently approximate expectations \mathbb{E}_p w.r.t. the EBM $p(y|x; \theta)$,

$$\mathbb{E}_p[\xi(y)] = \int \xi(y) p(y|x; \theta) dy \approx \sum_{m=1}^M w^{(m)} \xi(y^{(m)}), \quad (7)$$

$$w^{(m)} = \frac{e^{f_\theta(x, y^{(m)})} / q(y^{(m)}|x; \phi)}{\sum_{l=1}^M e^{f_\theta(x, y^{(l)})} / q(y^{(l)}|x; \phi)}.$$

Here, $\{y^{(m)}\}_{m=1}^M \sim q(y|x; \phi)$ are samples drawn from the MDN proposal, and $\xi(y)$ is the quantity over which we are taking the expectation. For example, setting $\xi(y) = y$ in (7) enables us to approximately compute the EBM mean. In this manner, we can thus directly produce a stand-alone prediction y^* for the EBM $p(y|x; \theta)$. Using the same technique, we can also estimate the variance of the EBM as a measure of its uncertainty.

Note that we can also draw approximate samples from the EBM $p(y|x; \theta)$ by re-sampling with replacement from the set $\{y^{(m)}\}_{m=1}^M \sim q(y|x; \phi)$ of proposal samples,

drawing each $y^{(m)}$ with probability $w^{(m)}$ (Rubin, 1987). We demonstrate this sampling technique in Figure S4 in the supplementary material. There, we observe that the technique produces accurate EBM samples even when the proposal is unimodal and thus not a particularly close approximation of the EBM.

3.3 Improved MDN Training

Lastly, we employ Result 1 to improve the training of MDNs $q(y|x; \phi)$. We simply extend our proposed approach for jointly training an EBM $p(y|x; \theta)$ and MDN proposal $q(y|x; \phi)$ from Section 3.2. Instead of defining the MDN by adding a network head onto the EBM (Figure 1), we now define $q(y|x; \phi)$ in terms of a full DNN g_ϕ , as illustrated in Figure 3. Now, we thus train two separate DNNs f_θ and g_ϕ . As in Section 3.2.1, we train the EBM $p(y|x; \theta)$ and MDN $q(y|x; \phi)$ jointly. At each iteration, we draw samples $\{y_i^{(m)}\}_{m=1}^M \sim q(y|x_i; \phi)$ and update θ via the loss $J_{\text{NCE}}(\theta)$ in (6). The EBM is thus trained using NCE with the MDN acting as a noise distribution. At each iteration, we also update the MDN parameters ϕ via the loss,

$$J_{\text{MDN}}(\phi) = \frac{1}{N} \sum_{i=1}^N \frac{1}{2} \log \left(\frac{1}{M} \sum_{m=1}^M \frac{e^{f_\theta(x_i, y_i^{(m)})}}{q(y_i^{(m)}|x_i; \phi)} \right) - \frac{1}{2} \log q(y_i|x_i; \phi). \quad (8)$$

The MDN $q(y|x; \phi)$ is thus trained by minimizing a sum of its NLL $-\log q(y_i|x_i; \phi)$ and the $J_{\text{KL}}(\theta)$ loss in (5). Compared to conventional MDN training, we thus employ our approximation of $D_{\text{KL}}(p \parallel q)$ as an additional loss, guiding $q(y|x; \phi)$ towards the EBM $p(y|x; \theta)$.

In contrast to MDNs, EBMs are not restricted to distributions which are convenient to evaluate and sample. The EBM $p(y|x; \theta)$ is thus generally a more flexible model than $q(y|x; \phi)$ and therefore able to better approximate the underlying true distribution $p(y|x)$. Compared to MDNs, which define a distribution $q(y|x; \phi)$ by mapping x to the set $\{\pi_\phi^{(k)}, \mu_\phi^{(k)}, \sigma_\phi^{(k)}\}_{k=1}^K$, the EBM $p(y|x; \theta) = e^{f_\theta(x, y)} / \int e^{f_\theta(x, \tilde{y})} d\tilde{y}$ also offers a more direct representation of the distribution via its scalar function $f_\theta(x, y)$, potentially leading to a more straightforward learning problem. Therefore, we argue that guiding the MDN $q(y|x; \phi)$ towards the EBM $p(y|x; \theta)$ during training via the loss $J_{\text{MDN}}(\phi)$ in (8) should help mitigate some of the known inefficiencies of MDN training. We note that our proposed joint training approach is twice as slow compared to conventional MDN training, as two separate DNNs f_θ and g_ϕ are updated at each iteration. After training, the EBM can however be discarded and does therefore not affect the computational cost of the MDN at test-time.

4 RELATED WORK

Our proposed approach to automatically learn a proposal during EBM training is related to the work of (Kim and Bengio, 2016; Zhai et al., 2016; Kumar et al., 2019; Grathwohl et al., 2021), training EBMs for generative modelling tasks by jointly learning an auxiliary sampler via adversarial training. We instead train conditional EBMs for regression and are able to derive a particularly convenient KL divergence approximation (Result 1).

Our approach is also inspired by the concept of cooperative learning (Xie et al., 2018a,b, 2021c,b), which entails jointly training an EBM and a generator network via Markov chain Monte Carlo (MCMC) teaching. Specifically, the generator serves as a proposal and provides initial samples which are refined via MCMC to approximately sample from the EBM, training the EBM via contrastive divergence. Then, the generator network is trained to match these refined MCMC samples using a standard regression loss. Cooperative learning has recently also been extended to train EBMs for conditional generative modelling tasks (Xie et al., 2021a; Zhang et al., 2021). While our proposed method also entails jointly training conditional EBMs and proposals, we specifically study the important application of low-dimensional regression. In this setting, MCMC-based training of EBMs has been shown highly inefficient (Gustafsson et al., 2020b). By deriving Result 1, we can instead employ the more effective training method of NCE, and train the proposal by directly minimizing its KL divergence to the EBM. Since MCMC is not employed, our proposed method is also computationally efficient, and very simple to implement, compared to cooperative learning.

Our method to improve the training of an MDN by guiding it towards an EBM is related to (Gao et al., 2020), who train a generative flow-based model jointly with an EBM through a minimax game. In contrast, our joint training method is non-adversarial and can even be implemented by directly minimizing one unified objective. On a conceptual level, our MDN training approach is also related to work on teacher-student networks and knowledge distillation (Hinton et al., 2015; Mirzadeh et al., 2020; Xu et al., 2020; Ding et al., 2021a). In a knowledge distillation problem, a teacher network is utilized to improve the performance of a more lightweight student network. While knowledge distillation for regression is not a particularly well-studied topic, it has been studied for image-based regression tasks in very recent work (Ding et al., 2021a). A student network is there enhanced by augmenting its training set with images and pseudo targets generated by a conditional GAN and a pre-trained teacher network, respectively.

Table 1: Results for the EBM 1D regression experiments. Results are in terms of approximate KL divergence for the first dataset (Gustafsson et al., 2020b), and in terms of approximate NLL for the second (Brando et al., 2019).

Dataset	NCE					Ours		
	$\sigma_1=0.05$	$\sigma_1=0.1$	$\sigma_1=0.2$	$\sigma_1=0.4$	$\sigma_1=0.8$	$K=1$	$K=4$	$K=16$
Gustafsson et al. (2020b)	0.042	0.036	0.040	0.042	0.042	0.038	0.032	0.035
Brando et al. (2019)	2.30	1.98	1.72	1.67	1.70	1.69	1.67	1.65

Table 2: Results in terms of approximate NLL for the EBM steering angle prediction experiments.

		NCE			Ours
$\sigma_1=0.1, \sigma_2=20$	$\sigma_1=1, \sigma_2=20$	$\sigma_1=2, \sigma_2=20$	$\sigma_1=1, \sigma_2=10$	$\sigma_1=1, \sigma_2=40$	$K=4$
1.59 ± 0.08	1.51 ± 0.05	1.56 ± 0.04	2.03 ± 0.14	1.39 ± 0.02	1.58 ± 0.13

In contrast, our approach entails distilling the conditional EBM distribution $p(y|x; \theta)$ into a student MDN for each example in the original training set. Furthermore, our approach trains the teacher EBM and student MDN jointly, where the student MDN generates proposal samples used for training the EBM teacher.

5 EXPERIMENTS

We perform comprehensive experiments on illustrative 1D regression problems and four image-based regression tasks, which are all detailed below. We first evaluate our proposed method for automatically learning an effective proposal during EBM training in Section 5.1. There, we compare our EBM training method with NCE, achieving highly competitive performance across all five tasks without having to tune any task-dependent hyperparameters. In Section 5.2, we then evaluate our proposed approach for training MDNs. Compared to conventional MDN training, we consistently obtain improved test log-likelihoods. All experiments are implemented in PyTorch (Paszke et al., 2019). Example model and training code is found in the supplementary material, and our complete implementation is also made publicly available. All models were trained on individual NVIDIA TITAN Xp GPUs.

1D Regression We study two illustrative 1D regression problems with $x \in \mathbb{R}$ and $y \in \mathbb{R}$. The first dataset is specified in (Gustafsson et al., 2020b) and contains 2000 training examples. It is visualized in Figure 2. The second dataset is specified in (Brando et al., 2019), containing 1900 test examples and 1700 examples for training.

Steering Angle Prediction Here, we are given an image x from a forward-facing camera mounted inside of a car. The task is to predict the corresponding steering angle $y \in \mathbb{R}$ of the car at that moment. We utilize the dataset from (Ding et al., 2021b, 2020),

containing 12271 examples. We randomly split the dataset into training (80%) and test (20%) sets. All images x are of size 64×64 .

Cell-Count Prediction Given a synthetic fluorescence microscopy image x , the task is here to predict the number of cells $y \in \mathbb{R}_+$ in the image. We utilize the dataset from (Ding et al., 2021b, 2020), which consists of 200000 grayscale images of size 64×64 . From this dataset, we randomly draw 10000 images each to construct training and test sets. An example image x is visualized in Figure 1.

Age Estimation In age estimation, we are given an image x of a person’s face and are tasked with predicting the age $y \in \mathbb{R}_+$ of this person. We utilize the UTKFace (Zhang et al., 2017) dataset, specifically the processed version provided by Ding et al. (2021b, 2020). This dataset contains 14760 examples, which we randomly split into training (80%) and test (20%) sets. All images x are of size 64×64 .

Head-Pose Estimation In this case, we are given an image x of a person, and the task is to predict the orientation $y \in \mathbb{R}^3$ of this person’s head. Here, y is the yaw, pitch and roll angles of the head. We utilize the BIWI (Fanelli et al., 2013) dataset, specifically the processed version provided by Yang et al. (2019). We employ protocol 2 as defined in (Yang et al., 2019), giving 5065 test images and 10613 images for training. All images x are of size 64×64 .

5.1 EBM Experiments

We first evaluate our proposed method for automatically learning an effective proposal during EBM training, by performing extensive experiments on all five regression tasks.

1D Regression The EBM DNN $f_\theta(x, y)$ is here a simple feed-forward network, taking $x \in \mathbb{R}$ and $y \in \mathbb{R}$ as inputs. Separate sets of fully-connected layers ex-

Table 3: Results in terms of approximate NLL for the EBM cell-count prediction experiments.

		NCE			Ours
$\sigma_1=0.1, \sigma_2=40$	$\sigma_1=1, \sigma_2=40$	$\sigma_1=2, \sigma_2=40$	$\sigma_1=1, \sigma_2=20$	$\sigma_1=1, \sigma_2=80$	$K=4$
2.71±0.07	2.64±0.05	2.65±0.05	3.12±0.37	2.70±0.05	2.66±0.03

Table 4: Results in terms of approximate NLL for the EBM age estimation experiments.

		NCE			Ours
$\sigma_1=0.01, \sigma_2=20$	$\sigma_1=0.1, \sigma_2=20$	$\sigma_1=1, \sigma_2=20$	$\sigma_1=0.1, \sigma_2=10$	$\sigma_1=0.1, \sigma_2=40$	$K=4$
4.18±0.30	3.81±0.18	4.13±0.48	3.97±0.21	4.47±0.25	4.30±0.30

tract features $h_x \in \mathbb{R}^{10}$ from x and $h_y \in \mathbb{R}^{10}$ from y . The two feature vectors are then concatenated and processed to output $f_\theta(x, y) \in \mathbb{R}$. The MDN network head $g_\phi(x)$ takes the feature $h_x \in \mathbb{R}^{10}$ as input and outputs $\{\pi_\phi^{(k)}, \mu_\phi^{(k)}, \sigma_\phi^{(k)}\}_{k=1}^K$. We use the ADAM (Kingma and Ba, 2014) optimizer to jointly train f_θ and g_ϕ . For the first dataset, we follow (Gustafsson et al., 2020b) and evaluate the training methods in terms of how close the EBM $p(y|x; \theta)$ is to the known ground truth $p(y|x)$, as measured by the (approximately computed) KL divergence. For the second dataset (Brando et al., 2019) we approximately compute the test set NLL of the EBM $p(y|x; \theta)$, by evaluating $f_\theta(x, y)$ at densely sampled y values in an interval $[y_{\min}, y_{\max}]$. We compare our proposed approach with training the EBM using NCE, employing the noise distribution $q(y) = \frac{1}{2} \sum_{k=1}^2 \mathcal{N}(y; y_i, \sigma_k^2 I)$. Following (Gustafsson et al., 2020b), we set $\sigma_1 = 0.1$, $\sigma_2 = 8\sigma_1$. We also report results for the values $\sigma_1 \in \{0.05, 0.2, 0.4, 0.8\}$. For our proposed approach, we report results for using $K \in \{1, 4, 16\}$ components in the MDN proposal. We train 20 networks for each setting and dataset, and report the mean of the 5 best runs. The results are found in Table 1. We observe that our proposed training method achieves highly competitive performance for all values of K . For NCE, the performance varies quite significantly with σ_1 , which would have to be tuned for each dataset.

Image-Based Regression We employ a virtually identical network architecture for all four image-based regression tasks, only making minor modifications for the head-pose estimation task to accommodate the higher target dimension $y \in \mathbb{R}^3$. The EBM DNN $f_\theta(x, y)$ is composed of a ResNet18 (He et al., 2016) that extracts features $h_x \in \mathbb{R}^{512}$ from the input image x . From the target y , fully-connected layers extract features $h_y \in \mathbb{R}^{128}$. After concatenation of h_x and h_y , fully-connected layers then output $f_\theta(x, y) \in \mathbb{R}$. The MDN network head $g_\phi(x)$ takes the image features $h_x \in \mathbb{R}^{512}$ as input and outputs $\{\pi_\phi^{(k)}, \mu_\phi^{(k)}, \sigma_\phi^{(k)}\}_{k=1}^K$. Again, we use ADAM to jointly train f_θ and g_ϕ . We

evaluate the training methods by approximately computing the test set NLL of the EBM $p(y|x; \theta)$. We compare our proposed approach with training the EBM using NCE, employing the noise distribution $q(y) = \frac{1}{2} \sum_{k=1}^2 \mathcal{N}(y; y_i, \sigma_k^2 I)$. For each of the four tasks, we initially set $\{\sigma_1, \sigma_2\}$ to what was used for age estimation and head-pose estimation in (Gustafsson et al., 2020a) and then carefully tune them further. Based on the 1D regression results in Table 1, we use $K = 4$ components in the MDN proposal for our proposed approach. We train 20 networks for each setting and dataset, and report the mean of the 5 best runs. The results are found in Table 2 to Table 5. We observe that our proposed training method achieves highly competitive performance. In particular, our method significantly outperforms the NCE baseline on the more challenging head-pose estimation task (Table 5), which has a multi-dimensional target space. Note that we use an identical architecture for the MDN proposal in our training method across all four tasks, while the task-dependent NCE hyperparameters $\{\sigma_1, \sigma_2\}$ are tuned directly on each of the corresponding *test* sets. Thus, NCE is here a very strong baseline.

5.2 MDN Experiments

Lastly, we perform experiments on the four image-based regression tasks to evaluate our proposed approach for training MDNs $q(y|x; \phi)$. For the EBM DNN $f_\theta(x, y)$, an identical network architecture is used as in the EBM experiments (Section 5.1). The MDN network $g_\phi(x)$ is now a full DNN. It consists of a ResNet18 that extracts image features $h_x \in \mathbb{R}^{512}$, and a head of fully-connected layers that takes $h_x \in \mathbb{R}^{512}$ as input and outputs $\{\pi_\phi^{(k)}, \mu_\phi^{(k)}, \sigma_\phi^{(k)}\}_{k=1}^K$. As described in Section 3.3, the MDN DNN g_ϕ is trained by minimizing the loss $J_{\text{MDN}}(\phi)$ in (8), whereas f_θ is trained via $J_{\text{NCE}}(\theta)$ in (6). As in the previous experiments, ADAM is used to jointly train f_θ and g_ϕ . We compare our proposed approach with the conventional MDN training method, i.e. minimizing the NLL $\sum_{i=1}^N -\log q(y_i|x_i; \phi)$. We evaluate the training methods in terms of test set NLL,

Table 5: Results in terms of approximate NLL for the EBM head-pose estimation experiments.

		NCE			Ours
$\sigma_1 = 0.1, \sigma_2 = 20$	$\sigma_1 = 1, \sigma_2 = 20$	$\sigma_1 = 2, \sigma_2 = 20$	$\sigma_1 = 1, \sigma_2 = 10$	$\sigma_1 = 1, \sigma_2 = 40$	$K = 4$
13.68 ± 0.10	10.99 ± 0.29	10.85 ± 0.11	10.73 ± 0.19	11.20 ± 0.15	9.51 ± 0.07

Table 6: Results in terms of NLL for the MDN experiments on four image-based regression tasks.

Task	NLL			Ours		
	$K = 4$	$K = 8$	$K = 16$	$K = 4$	$K = 8$	$K = 16$
Steering angle	1.45 ± 0.13	1.25 ± 0.05	-	1.00 ± 0.03	1.01 ± 0.04	-
Cell-count	2.80 ± 0.09	2.90 ± 0.06	-	2.80 ± 0.06	2.75 ± 0.06	-
Age	4.88 ± 0.21	4.71 ± 0.35	-	3.57 ± 0.28	3.65 ± 0.18	-
Head-pose	11.02 ± 0.16	10.68 ± 0.39	10.71 ± 0.17	8.69 ± 0.10	8.79 ± 0.06	8.77 ± 0.09

for MDNs with $K \in \{4, 8, 16\}$ components. We train 20 networks for each setting and dataset, and report the mean of the 5 best runs. The results are found in Table 6. We observe that our proposed training method consistently outperforms the baseline of pure NLL training. For the steering angle prediction and age estimation tasks, our approach achieves substantial improvements. Moreover, in the particularly challenging head-pose estimation task, our approach outperforms the standard MDN by a significant margin.

6 CONCLUSION

We derived an efficient and convenient objective that can be employed to train a parameterized distribution $q(y|x; \phi)$ by minimizing its KL divergence to a conditional EBM $p(y|x; \theta)$. We then applied the derived objective to jointly learn an effective MDN proposal distribution during EBM training, thus addressing the main practical limitations of energy-based regression. We evaluated our proposed EBM training method on illustrative 1D regression problems and real-world regression tasks within computer vision, achieving highly competitive performance without having to tune any task-dependent hyperparameters. Lastly, we employed the derived objective to improve training of stand-alone MDNs, consistently obtaining more accurate predictive distributions compared to conventional MDN training. Future directions include estimating the EBM uncertainty via test-time use of the trained MDN proposal, and applying our MDN training approach to additional tasks.

Acknowledgements

This research was supported by the Swedish Foundation for Strategic Research via the project *ASSEMBLE* (contract number: RIT15-0012), by the Swedish Research Council via the project *NewLEADS - New*

Directions in Learning Dynamical Systems (contract number: 621-2016-06079), and by the *Kjell & Märta Beijer Foundation*.

References

- F. Bao, C. Li, K. Xu, H. Su, J. Zhu, and B. Zhang. Bi-level score matching for learning energy-based latent variable models. In *Advances in Neural Information Processing Systems (NeurIPS)*, 2020.
- Y. Bengio, R. Ducharme, P. Vincent, and C. Jauvin. A neural probabilistic language model. *Journal of machine learning research*, 3(Feb):1137–1155, 2003.
- C. M. Bishop. Mixture density networks, 1994.
- A. Brando, J. A. Rodríguez-Serrano, J. Vitria, and A. Rubio. Modelling heterogeneous distributions with an uncountable mixture of asymmetric laplacians. In *Advances in Neural Information Processing Systems (NeurIPS)*, 2019.
- K. Chua, R. Calandra, R. McAllister, and S. Levine. Deep reinforcement learning in a handful of trials using probabilistic dynamics models. In *Advances in Neural Information Processing Systems (NeurIPS)*, pages 4759–4770, 2018.
- H. Cui, V. Radosavljevic, F.-C. Chou, T.-H. Lin, T. Nguyen, T.-K. Huang, J. Schneider, and N. Djuric. Multimodal trajectory predictions for autonomous driving using deep convolutional networks. In *International Conference on Robotics and Automation (ICRA)*, pages 2090–2096. IEEE, 2019.
- M. Danelljan, L. V. Gool, and R. Timofte. Probabilistic regression for visual tracking. In *Proceedings of the IEEE/CVF Conference on Computer Vision and Pattern Recognition (CVPR)*, pages 7183–7192, 2020.
- X. Ding, Y. Wang, Z. Xu, W. J. Welch, and Z. J. Wang. Continuous conditional generative adversarial networks for image generation: Novel losses and label

- input mechanisms. *arXiv preprint arXiv:2011.07466*, 2020.
- X. Ding, Y. Wang, Z. Xu, Z. J. Wang, and W. J. Welch. Distilling and transferring knowledge via cGAN-generated samples for image classification and regression. *arXiv preprint arXiv:2104.03164*, 2021a.
- X. Ding, Y. Wang, Z. Xu, W. J. Welch, and Z. J. Wang. CcGAN: Continuous conditional generative adversarial networks for image generation. In *International Conference on Learning Representations (ICLR)*, 2021b. URL <https://openreview.net/forum?id=Przjug0sDeE>.
- Y. Du and I. Mordatch. Implicit generation and modeling with energy based models. In *Advances in Neural Information Processing Systems (NeurIPS)*, 2019.
- Y. Du, S. Li, J. Tenenbaum, and I. Mordatch. Improved contrastive divergence training of energy based models. In *International Conference on Machine Learning (ICML)*, 2021.
- G. Fanelli, M. Dantone, J. Gall, A. Fossati, and L. Van Gool. Random forests for real time 3d face analysis. *International Journal of Computer Vision (IJCV)*, 101(3):437–458, 2013.
- P. Florence, C. Lynch, A. Zeng, O. A. Ramirez, A. Wahid, L. Downs, A. Wong, J. Lee, I. Mordatch, and J. Tompson. Implicit behavioral cloning. In *The 5th Annual Conference on Robot Learning (CoRL)*, 2021.
- R. Gao, Y. Lu, J. Zhou, S.-C. Zhu, and Y. Nian Wu. Learning generative convnets via multi-grid modeling and sampling. In *Proceedings of the IEEE Conference on Computer Vision and Pattern Recognition (CVPR)*, pages 9155–9164, 2018.
- R. Gao, E. Nijkamp, D. P. Kingma, Z. Xu, A. M. Dai, and Y. N. Wu. Flow contrastive estimation of energy-based models. In *Proceedings of the IEEE/CVF Conference on Computer Vision and Pattern Recognition (CVPR)*, pages 7518–7528, 2020.
- J. Gast and S. Roth. Lightweight probabilistic deep networks. In *Proceedings of the IEEE Conference on Computer Vision and Pattern Recognition (CVPR)*, pages 3369–3378, 2018.
- W. Grathwohl, K.-C. Wang, J.-H. Jacobsen, D. Duvenaud, M. Norouzi, and K. Swersky. Your classifier is secretly an energy based model and you should treat it like one. In *International Conference on Learning Representations (ICLR)*, 2020.
- W. S. Grathwohl, J. J. Kelly, M. Hashemi, M. Norouzi, K. Swersky, and D. Duvenaud. No MCMC for me: Amortized sampling for fast and stable training of energy-based models. In *International Conference on Learning Representations (ICLR)*, 2021.
- F. K. Gustafsson, M. Danelljan, G. Bhat, and T. B. Schön. Energy-based models for deep probabilistic regression. In *Proceedings of the European Conference on Computer Vision (ECCV)*, August 2020a.
- F. K. Gustafsson, M. Danelljan, R. Timofte, and T. B. Schön. How to train your energy-based model for regression. In *Proceedings of the British Machine Vision Conference (BMVC)*, September 2020b.
- F. K. Gustafsson, M. Danelljan, and T. B. Schön. Accurate 3D object detection using energy-based models. In *Proceedings of the IEEE/CVF Conference on Computer Vision and Pattern Recognition (CVPR) Workshops*, 2021.
- M. Gutmann and A. Hyvärinen. Noise-contrastive estimation: A new estimation principle for unnormalized statistical models. In *Proceedings of the International Conference on Artificial Intelligence and Statistics (AISTATS)*, pages 297–304, 2010.
- K. He, X. Zhang, S. Ren, and J. Sun. Deep residual learning for image recognition. In *Proceedings of the IEEE Conference on Computer Vision and Pattern Recognition (CVPR)*, pages 770–778, 2016.
- J. N. Hendriks, F. K. Gustafsson, A. H. Ribeiro, A. G. Wills, and T. B. Schön. Deep energy-based NARX models. In *Proceedings of the 19th IFAC Symposium on System Identification (SYSID)*, July 2021.
- G. Hinton, S. Osindero, M. Welling, and Y.-W. Teh. Unsupervised discovery of nonlinear structure using contrastive backpropagation. *Cognitive science*, 30(4):725–731, 2006.
- G. Hinton, O. Vinyals, and J. Dean. Distilling the knowledge in a neural network. *arXiv preprint arXiv:1503.02531*, 2015.
- L. U. Hjorth and I. T. Nabney. Regularisation of mixture density networks. In *1999 Ninth International Conference on Artificial Neural Networks ICANN 99 (Conf. Publ. No. 470)*, volume 2, pages 521–526. IET, 1999.
- E. Ilg, O. Cicek, S. Galesso, A. Klein, O. Makansi, F. Hutter, and T. Bro. Uncertainty estimates and multi-hypotheses networks for optical flow. In *Proceedings of the European Conference on Computer Vision (ECCV)*, pages 652–667, 2018.
- R. Jozefowicz, O. Vinyals, M. Schuster, N. Shazeer, and Y. Wu. Exploring the limits of language modeling. *arXiv preprint arXiv:1602.02410*, 2016.
- A. Kendall and Y. Gal. What uncertainties do we need in Bayesian deep learning for computer vision? In *Advances in Neural Information Processing Systems (NeurIPS)*, pages 5574–5584, 2017.

- T. Kim and Y. Bengio. Deep directed generative models with energy-based probability estimation. *arXiv preprint arXiv:1606.03439*, 2016.
- D. P. Kingma and J. Ba. Adam: A method for stochastic optimization. *arXiv preprint arXiv:1412.6980*, 2014.
- R. Kumar, S. Ozair, A. Goyal, A. Courville, and Y. Bengio. Maximum entropy generators for energy-based models. *arXiv preprint arXiv:1901.08508*, 2019.
- B. Lakshminarayanan, A. Pritzel, and C. Blundell. Simple and scalable predictive uncertainty estimation using deep ensembles. In *Advances in Neural Information Processing Systems (NeurIPS)*, pages 6402–6413, 2017.
- Y. LeCun, S. Chopra, R. Hadsell, M. Ranzato, and F. Huang. A tutorial on energy-based learning. *Predicting structured data*, 1(0), 2006.
- C. Li and G. H. Lee. Generating multiple hypotheses for 3d human pose estimation with mixture density network. In *Proceedings of the IEEE/CVF Conference on Computer Vision and Pattern Recognition (CVPR)*, pages 9887–9895, 2019.
- Z. Ma and M. Collins. Noise contrastive estimation and negative sampling for conditional models: Consistency and statistical efficiency. In *Proceedings of the Conference on Empirical Methods in Natural Language Processing (EMNLP)*, pages 3698–3707, 2018.
- O. Makansi, E. Ilg, O. Cicek, and T. Brox. Overcoming limitations of mixture density networks: A sampling and fitting framework for multimodal future prediction. In *Proceedings of the IEEE Conference on Computer Vision and Pattern Recognition (CVPR)*, pages 7144–7153, 2019.
- S. I. Mirzadeh, M. Farajtabar, A. Li, N. Levine, A. Matsukawa, and H. Ghasemzadeh. Improved knowledge distillation via teacher assistant. In *Proceedings of the AAAI Conference on Artificial Intelligence*, pages 5191–5198, 2020.
- A. Mnih and G. Hinton. Learning nonlinear constraints with contrastive backpropagation. In *Proceedings of the IEEE International Joint Conference on Neural Networks*, volume 2, pages 1302–1307. IEEE, 2005.
- K. Murphy, C. Esteves, V. Jampani, S. Ramalingam, and A. Makadia. Implicit-pdf: Non-parametric representation of probability distributions on the rotation manifold. In *International Conference on Machine Learning (ICML)*, 2021.
- E. Nijkamp, M. Hill, S.-C. Zhu, and Y. N. Wu. Learning non-convergent non-persistent short-run mcmc toward energy-based model. In *Advances in Neural Information Processing Systems (NeurIPS)*, pages 5233–5243, 2019.
- M. Osadchy, M. L. Miller, and Y. L. Cun. Synergistic face detection and pose estimation with energy-based models. In *Advances in Neural Information Processing Systems (NeurIPS)*, pages 1017–1024, 2005.
- A. B. Owen. *Monte Carlo theory, methods and examples*. 2013.
- B. Pang, T. Han, E. Nijkamp, S.-C. Zhu, and Y. N. Wu. Learning latent space energy-based prior model. In *Advances in Neural Information Processing Systems (NeurIPS)*, 2020.
- A. Paszke, S. Gross, F. Massa, A. Lerer, J. Bradbury, G. Chanan, T. Killeen, Z. Lin, N. Gimelshein, L. Antiga, et al. PyTorch: An imperative style, high-performance deep learning library. In *Advances in Neural Information Processing Systems (NeurIPS)*, pages 8024–8035, 2019.
- D. B. Rubin. The calculation of posterior distributions by data augmentation: Comment: A noniterative sampling/importance resampling alternative to the data augmentation algorithm for creating a few imputations when fractions of missing information are modest: The sir algorithm. *Journal of the American Statistical Association*, 82(398):543–546, 1987.
- C. Rupprecht, I. Laina, R. DiPietro, M. Baust, F. Tombari, N. Navab, and G. D. Hager. Learning in an uncertain world: Representing ambiguity through multiple hypotheses. In *Proceedings of the IEEE International Conference on Computer Vision (ICCV)*, pages 3591–3600, 2017.
- Y. Song and D. P. Kingma. How to train your energy-based models. *arXiv preprint arXiv:2101.03288*, 2021.
- Y. W. Teh, M. Welling, S. Osindero, and G. E. Hinton. Energy-based models for sparse overcomplete representations. *Journal of Machine Learning Research*, 4(Dec):1235–1260, 2003.
- A. Varamesh and T. Tuytelaars. Mixture dense regression for object detection and human pose estimation. In *Proceedings of the IEEE/CVF Conference on Computer Vision and Pattern Recognition (CVPR)*, pages 13086–13095, 2020.
- J. Xie, Y. Lu, S.-C. Zhu, and Y. Wu. A theory of generative convnet. In *International Conference on Machine Learning (ICML)*, pages 2635–2644, 2016.
- J. Xie, S.-C. Zhu, and Y. Nian Wu. Synthesizing dynamic patterns by spatial-temporal generative convnet. In *Proceedings of the IEEE Conference on Computer Vision and Pattern Recognition (CVPR)*, pages 7093–7101, 2017.
- J. Xie, Y. Lu, R. Gao, and Y. N. Wu. Cooperative learning of energy-based model and latent variable model via MCMC teaching. In *Proceedings*

of the *AAAI Conference on Artificial Intelligence*, volume 32, 2018a.

- J. Xie, Y. Lu, R. Gao, S.-C. Zhu, and Y. N. Wu. Cooperative training of descriptor and generator networks. *IEEE Transactions on Pattern Analysis and Machine Intelligence (TPAMI)*, 42(1):27–45, 2018b.
- J. Xie, Z. Zheng, R. Gao, W. Wang, S.-C. Zhu, and Y. N. Wu. Learning descriptor networks for 3d shape synthesis and analysis. In *Proceedings of the IEEE Conference on Computer Vision and Pattern Recognition (CVPR)*, pages 8629–8638, 2018c.
- J. Xie, Z. Zheng, X. Fang, S.-C. Zhu, and Y. N. Wu. Cooperative training of fast thinking initializer and slow thinking solver for conditional learning. *IEEE Transactions on Pattern Analysis and Machine Intelligence (TPAMI)*, 2021a.
- J. Xie, Z. Zheng, X. Fang, S.-C. Zhu, and Y. N. Wu. Learning cycle-consistent cooperative networks via alternating mcmc teaching for unsupervised cross-domain translation. In *The Thirty-Fifth AAAI Conference on Artificial Intelligence (AAAI)*, 2021b.
- J. Xie, Z. Zheng, and P. Li. Learning energy-based model with variational auto-encoder as amortized sampler. In *The Thirty-Fifth AAAI Conference on Artificial Intelligence (AAAI)*, volume 2, 2021c.
- G. Xu, Z. Liu, X. Li, and C. C. Loy. Knowledge distillation meets self-supervision. In *Proceedings of the European Conference on Computer Vision (ECCV)*, pages 588–604, 2020.
- T.-Y. Yang, Y.-T. Chen, Y.-Y. Lin, and Y.-Y. Chuang. FSA-Net: Learning fine-grained structure aggregation for head pose estimation from a single image. In *Proceedings of the IEEE Conference on Computer Vision and Pattern Recognition (CVPR)*, pages 1087–1096, 2019.
- S. Zhai, Y. Cheng, R. Feris, and Z. Zhang. Generative adversarial networks as variational training of energy based models. *arXiv preprint arXiv:1611.01799*, 2016.
- J. Zhang, J. Xie, Z. Zheng, and N. Barnes. Energy-based generative cooperative saliency prediction. *arXiv preprint arXiv:2106.13389*, 2021.
- Z. Zhang, Y. Song, and H. Qi. Age progression/regression by conditional adversarial autoencoder. In *Proceedings of the IEEE Conference on Computer Vision and Pattern Recognition (CVPR)*, pages 5810–5818, 2017. URL <https://susanqq.github.io/UTKFace/>.
- Y. Zhou, J. Gao, and T. Asfour. Movement primitive learning and generalization: Using mixture density networks. *IEEE Robotics & Automation Magazine*, 27(2):22–32, 2020.

Supplementary Material: Learning Proposals for Practical Energy-Based Regression

In this supplementary material, we provide additional details and results. It consists of Appendix A - Appendix G. After discussing limitations and societal impacts in Appendix A, we provide implementation details in Appendix B. Then, we describe all utilized datasets more closely in Appendix C. We then provide a complete derivation of Result 1 in Appendix D. Additional results for the 1D regression task is then provided in Appendix E. Lastly, Appendix F and Appendix G contain example model and training code. Note that figures in this supplementary material are numbered with the prefix "S". Numbers without this prefix refer to the main paper.

A LIMITATIONS & SOCIETAL IMPACTS

Our approach is primarily intended for regression tasks, where the target space has a limited number of dimensions. For each training sample, several target values are sampled from the proposal distribution. Our approach is therefore not intended to scale to very high-dimensional generative modeling tasks, such as image generation.

Training an EBM using our proposed method in Section 3.2 is somewhat slower than using the NCE baseline method, since we also have to update an MDN proposal at each iteration. The NCE baseline however requires hyperparameters to be tuned specifically for each task at hand. The *total* environmental impact due to training is therefore likely smaller for our proposed method. Our proposed approach for training MDNs in Section 3.3 does however not offer similar benefits compared to conventional MDN training, and is twice as slow to train. This issue would be mitigated to a certain extent by sharing parts of the network among the EBM and MDN, which could be explored in future work.

B IMPLEMENTATION DETAILS

We train all networks for 75 epochs with a batch size of 32. The number of samples M is always set to $M = 1024$. All networks are trained on individual NVIDIA TITAN Xp GPUs. Training 20 networks for a specific setting and dataset on one such GPU takes at most 24 – 48 hours. Producing the results in Table 1 to Table 6 thus required approximately 50 GPU days of training. We utilized an internal GPU cluster.

PyTorch code defining the network architecture used for the head-pose estimation task in Section 5.1 is found in Appendix F below. PyTorch code for the corresponding main training loop is found in Appendix G.

In Section 5.1, the EBM $p(y|x; \theta) = e^{f_\theta(x,y)} / \int e^{f_\theta(x,\tilde{y})} d\tilde{y}$ is evaluated by approximately computing its test set negative log-likelihood (NLL). We do so by evaluating $f_\theta(x,y)$ at densely sampled y values in an interval $[y_{\min}, y_{\max}]$. For the second 1D regression dataset, we evaluate at 8192 values in $[-12.5, 12.5]$. For steering angle prediction, 20000 values in $[-100, 100]$. For cell-count prediction, 19900 values in $[1, 200]$. For age estimation, 5900 values in $[1, 60]$. For head-pose estimation, 27000 values in $\{x \in \mathbb{R}^3 : x_i \in [-80, 80], i = 1, 2, 3\}$.

C DATASET DETAILS

The training data for the two 1D regression problems is visualized in Figure S1 and Figure S2.

For steering angle prediction, cell-count prediction and age estimation, our utilized datasets from (Ding et al., 2021b, 2020) are all available at https://github.com/UBCDingXin/improved_CcGAN.

The original age estimation dataset UTKFace (Zhang et al., 2017) is available at <https://susanqq.github.io/UTKFace/>, for non-commercial research purposes only. The dataset consists of images collected from the internet, i.e. images collected without explicitly obtained consent to be used specifically for training age estimation models. Thus, we choose to not display any dataset examples.

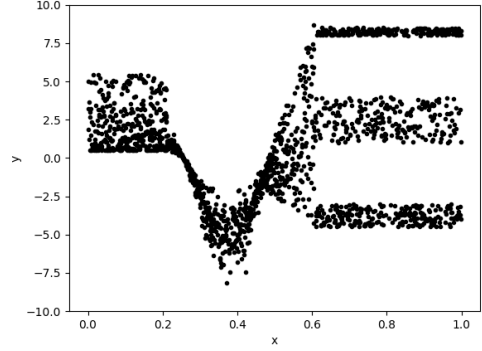
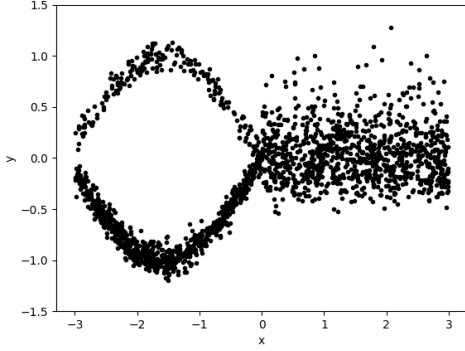


Figure S1: Training data $\{(x_i, y_i)\}_{i=1}^{2000}$ for the first 1D regression dataset (Gustafsson et al., 2020b). Figure S2: Training data $\{(x_i, y_i)\}_{i=1}^{1700}$ for the second 1D regression dataset (Brando et al., 2019).

For head-pose estimation, the BIWI (Fanelli et al., 2013) dataset is available for research purposes only. The dataset was created by recording 20 people (research subjects) while they freely turned their heads around. The processed version provided by Yang et al. (2019) that we utilize is available at <https://github.com/shamangary/FSA-Net>. Since the dataset images could potentially contain personally identifiable information, we choose to not display any dataset examples.

D DERIVATION OF RESULT 1

To derive Result 1 in Section 3.1, we first rewrite $\nabla_{\phi} D_{\text{KL}}(p(y|x; \theta) \parallel q(y|x; \phi))$ according to,

$$\begin{aligned}
 \nabla_{\phi} D_{\text{KL}}(p(y|x; \theta) \parallel q(y|x; \phi)) &= \nabla_{\phi} \int p(y|x; \theta) \log \frac{p(y|x; \theta)}{q(y|x; \phi)} dy \\
 &= \int p(y|x; \theta) \nabla_{\phi} \log \frac{p(y|x; \theta)}{q(y|x; \phi)} dy \\
 &= \int p(y|x; \theta) \nabla_{\phi} \left(\log p(y|x; \theta) - \log q(y|x; \phi) \right) dy \\
 &= - \int p(y|x; \theta) \nabla_{\phi} \log q(y|x; \phi) dy \\
 &= - \int p(y|x; \theta) \frac{1}{q(y|x; \phi)} \nabla_{\phi} q(y|x; \phi) dy \\
 &= - \int \frac{e^{f_{\theta}(x, y)}}{\int e^{f_{\theta}(x, \tilde{y})} d\tilde{y}} \frac{1}{q(y|x; \phi)} \nabla_{\phi} q(y|x; \phi) dy \\
 &= - \frac{1}{\int e^{f_{\theta}(x, \tilde{y})} d\tilde{y}} \int e^{f_{\theta}(x, y)} \frac{1}{q(y|x; \phi)} \nabla_{\phi} q(y|x; \phi) dy.
 \end{aligned}$$

Then, we approximate the two integrals using Monte Carlo importance sampling,

$$\begin{aligned}
 \nabla_{\phi} D_{\text{KL}}(p(y|x; \theta) \parallel q(y|x; \phi)) &= - \frac{1}{\int e^{f_{\theta}(x, \tilde{y})} d\tilde{y}} \int e^{f_{\theta}(x, y)} \frac{1}{q(y|x; \phi)} \nabla_{\phi} q(y|x; \phi) dy \\
 &= - \frac{1}{\int e^{f_{\theta}(x, y)} dy} \int \frac{e^{f_{\theta}(x, y)}}{q(y|x; \phi)^2} (\nabla_{\phi} q(y|x; \phi)) q(y|x; \phi) dy \\
 &= - \frac{1}{\int \frac{e^{f_{\theta}(x, y)}}{q(y|x; \phi)} q(y|x; \phi) dy} \int \frac{e^{f_{\theta}(x, y)}}{q(y|x; \phi)^2} (\nabla_{\phi} q(y|x; \phi)) q(y|x; \phi) dy \\
 &\approx - \frac{1}{\frac{1}{M} \sum_{m=1}^M \frac{e^{f_{\theta}(x, y^{(m)})}}{q(y^{(m)}|x; \phi)}} \left(\frac{1}{M} \sum_{m=1}^M \frac{e^{f_{\theta}(x, y^{(m)})}}{q(y^{(m)}|x; \phi)^2} \nabla_{\phi} q(y^{(m)}|x; \phi) \right),
 \end{aligned}$$

where $\{y^{(m)}\}_{m=1}^M$ are M independent samples drawn from $q(y|x; \phi)$. Finally, we further rewrite the resulting expression according to,

$$\begin{aligned}
 \nabla_{\phi} D_{\text{KL}}(p(y|x; \theta) \parallel q(y|x; \phi)) &\approx -\frac{1}{\frac{1}{M} \sum_{m=1}^M \frac{e^{f_{\theta}(x, y^{(m)})}}{q(y^{(m)}|x; \phi)}} \left(\frac{1}{M} \sum_{m=1}^M \frac{e^{f_{\theta}(x, y^{(m)})}}{q(y^{(m)}|x; \phi)^2} \nabla_{\phi} q(y^{(m)}|x; \phi) \right) \\
 &= \frac{1}{\frac{1}{M} \sum_{m=1}^M \frac{e^{f_{\theta}(x, y^{(m)})}}{q(y^{(m)}|x; \phi)}} \left(\frac{1}{M} \sum_{m=1}^M e^{f_{\theta}(x, y^{(m)})} \nabla_{\phi} \frac{1}{q(y^{(m)}|x; \phi)} \right) \\
 &= \frac{1}{\frac{1}{M} \sum_{m=1}^M \frac{e^{f_{\theta}(x, y^{(m)})}}{q(y^{(m)}|x; \phi)}} \left(\frac{1}{M} \sum_{m=1}^M \nabla_{\phi} \frac{e^{f_{\theta}(x, y^{(m)})}}{q(y^{(m)}|x; \phi)} \right) \\
 &= \frac{1}{\frac{1}{M} \sum_{m=1}^M \frac{e^{f_{\theta}(x, y^{(m)})}}{q(y^{(m)}|x; \phi)}} \nabla_{\phi} \left(\frac{1}{M} \sum_{m=1}^M \frac{e^{f_{\theta}(x, y^{(m)})}}{q(y^{(m)}|x; \phi)} \right) \\
 &= \left(\frac{1}{M} \sum_{m=1}^M \frac{e^{f_{\theta}(x, y^{(m)})}}{q(y^{(m)}|x; \phi)} \right)^{-1} \nabla_{\phi} \left(\frac{1}{M} \sum_{m=1}^M \frac{e^{f_{\theta}(x, y^{(m)})}}{q(y^{(m)}|x; \phi)} \right) \\
 &= \nabla_{\phi} \log \left(\frac{1}{M} \sum_{m=1}^M \frac{e^{f_{\theta}(x, y^{(m)})}}{q(y^{(m)}|x; \phi)} \right).
 \end{aligned}$$

D.1 Best Possible Proposal

We here expand on the footnote on page 3 of the main paper. When training the EBM $p(y|x; \theta) = e^{f_{\theta}(x, y)}/Z(x, \theta)$ by minimizing the approximated NLL in (2), we wish to use the proposal $q(y|x; \phi)$ that yields the best possible NLL approximation. In general, this is achieved when the proposal equals the EBM, i.e. when $q(y|x; \phi) = p(y|x; \theta)$. To see why this is true, we set $q = p$ in (2),

$$\begin{aligned}
 J(\theta) &= \frac{1}{N} \sum_{i=1}^N \log \left(\frac{1}{M} \sum_{m=1}^M \frac{e^{f_{\theta}(x_i, y_i^{(m)})}}{q(y_i^{(m)})} \right) - f_{\theta}(x_i, y_i) \\
 &= \frac{1}{N} \sum_{i=1}^N \log \left(\frac{1}{M} \sum_{m=1}^M \frac{e^{f_{\theta}(x_i, y_i^{(m)})}}{p(y_i^{(m)}|x_i; \theta)} \right) - f_{\theta}(x_i, y_i) \\
 &= \frac{1}{N} \sum_{i=1}^N \log \left(\frac{1}{M} \sum_{m=1}^M \frac{e^{f_{\theta}(x_i, y_i^{(m)})}}{e^{f_{\theta}(x_i, y_i^{(m)})}/Z(x_i, \theta)} \right) - f_{\theta}(x_i, y_i) \\
 &= \frac{1}{N} \sum_{i=1}^N \log \left(\frac{1}{M} \sum_{m=1}^M Z(x_i, \theta) \right) - f_{\theta}(x_i, y_i) \\
 &= \frac{1}{N} \sum_{i=1}^N \log Z(x_i, \theta) - f_{\theta}(x_i, y_i) \\
 &= \frac{1}{N} \sum_{i=1}^N -\log \left(\frac{e^{f_{\theta}(x_i, y_i)}}{Z(x_i, \theta)} \right) \\
 &= \frac{1}{N} \sum_{i=1}^N -\log p(y_i|x_i; \theta),
 \end{aligned}$$

which corresponds to the exact NLL objective.

E ADDITIONAL RESULTS

Figure 2 in the main paper visualizes the fully trained EBM and MDN proposal, i.e. after 75 epochs of training. In Figure S3, we instead visualize the EBM and MDN after 5 (top row), 10, 15, 20 and 25 (bottom row) epochs

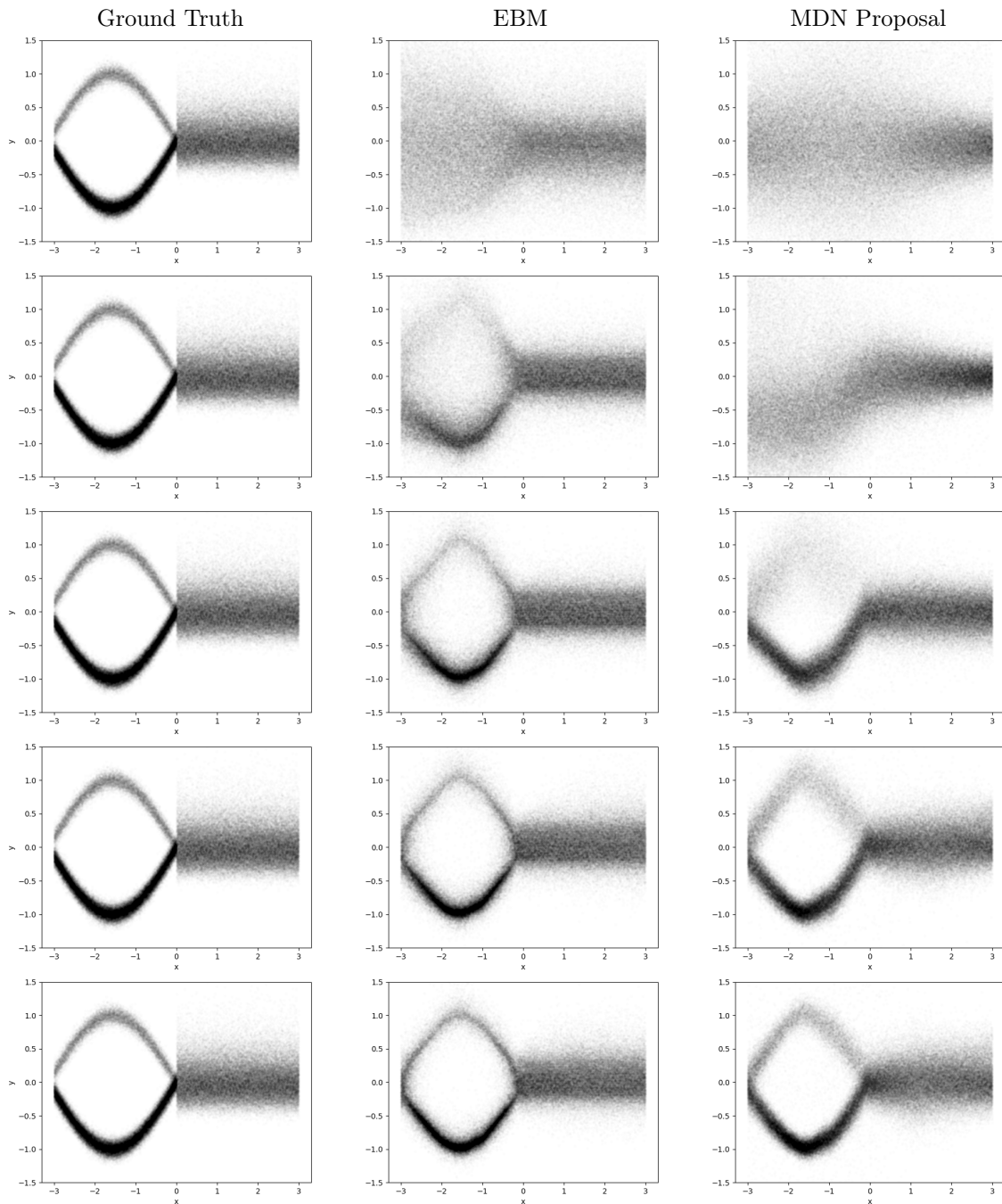


Figure S3: An illustrative 1D regression problem (Gustafsson et al., 2020b), demonstrating the effectiveness of our proposed method to jointly train an EBM $p(y|x; \theta)$ and MDN proposal $q(y|x; \phi)$. In this example, the MDN has $K = 4$ components. The EBM is trained using NCE with $q(y|x; \phi)$ acting as the noise distribution, whereas the MDN is trained by minimizing its KL divergence to $p(y|x; \theta)$. The EBM and MDN are here visualized after 5 (top row), 10, 15, 20 and 25 (bottom row) epochs of training.

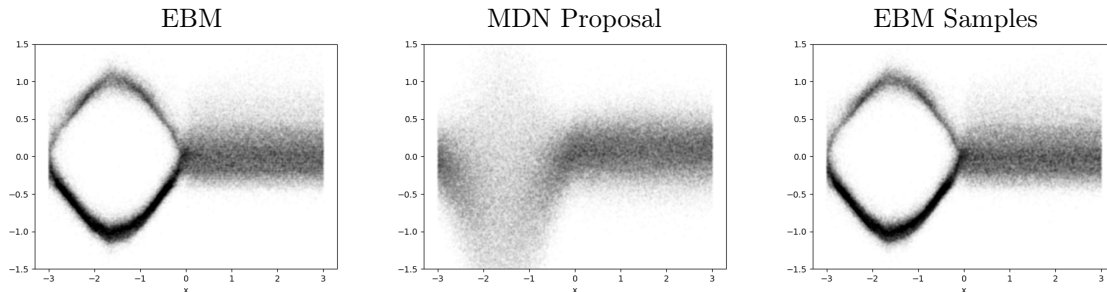


Figure S4: An illustrative 1D regression problem (Gustafsson et al., 2020b), demonstrating the effectiveness of our proposed method to jointly train an EBM $p(y|x; \theta)$ and MDN proposal $q(y|x; \phi)$. In this example, the MDN has $K = 1$ component. We here also demonstrate that we can draw approximate samples from the EBM using the method described in Section 3.2.2.

of training. We observe that the EBM is closer to the ground truth early on during training, guiding the MDN via the $J_{KL}(\phi)$ loss in (5).

In Figure S4, we visualize the fully trained EBM and MDN proposal when instead using just $K = 1$ component in the MDN. We observe that the EBM still is close to the ground truth. Apart from visualizing the EBM using the technique from (Gustafsson et al., 2020b) (evaluating $f_\theta(x, y)$ at densely sampled y values in the interval $[-3, 3]$ for each x), we here also demonstrate that we can draw approximate samples from the EBM using the method described in Section 3.2.2. For each x , we draw samples $\{y^{(m)}\}_{m=1}^{1024} \sim q(y|x; \phi)$ from the proposal, compute weights $\{w^{(m)}\}_{m=1}^{1024}$ according to (7), and then re-sample one value from this set $\{y^{(m)}\}_{m=1}^{1024}$ (drawing each $y^{(m)}$ with probability $w^{(m)}$). We observe in Figure S4 that this method produces accurate EBM samples, even when the proposal is unimodal and thus not a particularly close approximation of the EBM.

F PYTORCH CODE - NETWORK ARCHITECTURE

```
class NoiseNet(nn.Module):
    def __init__(self, hidden_dim):
        super().__init__()

        self.K = 4

        self.fc1_mean = nn.Linear(hidden_dim, hidden_dim)
        self.fc2_mean = nn.Linear(hidden_dim, 3*self.K)

        self.fc1_sigma = nn.Linear(hidden_dim, hidden_dim)
        self.fc2_sigma = nn.Linear(hidden_dim, 3*self.K)

        self.fc1_weight = nn.Linear(hidden_dim, hidden_dim)
        self.fc2_weight = nn.Linear(hidden_dim, self.K)

    def forward(self, x_feature):
        means = F.relu(self.fc1_mean(x_feature))
        means = self.fc2_mean(means)

        log_sigma2s = F.relu(self.fc1_sigma(x_feature))
        log_sigma2s = self.fc2_sigma(log_sigma2s)

        weight_logits = F.relu(self.fc1_weight(x_feature))
        weight_logits = self.fc2_weight(weight_logits)
        weights = torch.softmax(weight_logits, dim=1)
```

```
return means, log_sigma2s, weights
```

```
class PredictorNet(nn.Module):
    def __init__(self, input_dim, hidden_dim):
        super().__init__()

        self.fc1_y = nn.Linear(input_dim, 16)
        self.fc2_y = nn.Linear(16, 32)
        self.fc3_y = nn.Linear(32, 64)
        self.fc4_y = nn.Linear(64, 128)

        self.fc1_xy = nn.Linear(hidden_dim+128, hidden_dim)
        self.fc2_xy = nn.Linear(hidden_dim, 1)

    def forward(self, x_feature, y):
        batch_size, num_samples, _ = y.shape

        x_feature = x_feature.view(batch_size, 1, -1).expand(-1, num_samples, -1)
        x_feature = x_feature.reshape(batch_size*num_samples, -1)

        y = y.reshape(batch_size*num_samples, -1)

        y_feature = F.relu(self.fc1_y(y))
        y_feature = F.relu(self.fc2_y(y_feature))
        y_feature = F.relu(self.fc3_y(y_feature))
        y_feature = F.relu(self.fc4_y(y_feature))

        xy_feature = torch.cat([x_feature, y_feature], 1)

        xy_feature = F.relu(self.fc1_xy(xy_feature))
        score = self.fc2_xy(xy_feature)

        score = score.view(batch_size, num_samples)

    return score
```

```
class FeatureNet(nn.Module):
    def __init__(self):
        super().__init__()

        resnet18 = models.resnet18(pretrained=True)
        self.resnet18 = nn.Sequential(*list(resnet18.children())[:-2])

        self.avg_pool = nn.AdaptiveAvgPool2d((1, 1))

    def forward(self, x):
        x_feature = self.resnet18(x)
        x_feature = self.avg_pool(x_feature)
        x_feature = x_feature.squeeze(2).squeeze(2)

    return x_feature
```

```
class Net(nn.Module):
    def __init__(self):
        super(Net, self).__init__()
```

```

hidden_dim = 512

self.feature_net = FeatureNet()
self.noise_net = NoiseNet(hidden_dim)
self.predictor_net = PredictorNet(3, hidden_dim)

def forward(self, x, y):
    x_feature = self.feature_net(x)
    return self.noise_net(x_feature)

```

G PYTORCH CODE - TRAINING LOOP

```

for step, (xs, ys) in enumerate(train_loader):
    xs = xs.cuda() # (shape: (batch_size, 3, img_size, img_size))
    ys = ys.cuda() # (shape: (batch_size, 3))

    x_features = network.feature_net(xs) # (shape: (batch_size, hidden_dim))

    means, log_sigma2s, weights = network.noise_net(x_features.detach())
    # (means has shape: (batch_size, 3K))
    # (log_sigma2s has shape: (batch_size, 3K))
    # (weights has shape: (batch_size, K))
    sigmas = torch.exp(log_sigma2s/2.0) # (shape: (batch_size, 3K))
    means = means.view(-1, 3, K) # (shape: (batch_size, 3, K))
    sigmas = sigmas.view(-1, 3, K) # (shape: (batch_size, 3, K))

    q_distr = torch.distributions.normal.Normal(loc=means, scale=sigmas)
    q_ys_K = torch.exp(q_distr.log_prob(ys.unsqueeze(2)).sum(1)) # (shape: (batch_size, K))
    q_ys = torch.sum(weights*q_ys_K, dim=1) # (shape: (batch_size))

    y_samples_K = q_distr.sample(sample_shape=torch.Size([num_samples]))
    # (shape: (num_samples, batch_size, 3, K))
    inds = torch.multinomial(weights, num_samples=num_samples,
                             replacement=True).unsqueeze(2).unsqueeze(2)
    # (shape: (batch_size, num_samples, 1, 1))
    inds = inds.expand(-1, -1, 3, 1) # (shape: (batch_size, num_samples, 3, 1))
    inds = torch.transpose(inds, 1, 0) # (shape: (num_samples, batch_size, 3, 1))
    y_samples = y_samples_K.gather(3, inds).squeeze(3) # (shape: (num_samples, batch_size, 3))
    y_samples = y_samples.detach()
    q_y_samples_K = torch.exp(q_distr.log_prob(y_samples.unsqueeze(3)).sum(2))
    # (shape: (num_samples, batch_size, K))
    q_y_samples = torch.sum(weights.unsqueeze(0)*q_y_samples_K, dim=2)
    # (shape: (num_samples, batch_size))
    y_samples = torch.transpose(y_samples, 1, 0) # (shape: (batch_size, num_samples, 3))
    q_y_samples = torch.transpose(q_y_samples, 1, 0) # (shape: (batch_size, num_samples))

    scores_gt = network.predictor_net(x_features, ys.unsqueeze(1)) # (shape: (batch_size, 1))
    scores_gt = scores_gt.squeeze(1) # (shape: (batch_size))

    scores_samples = network.predictor_net(x_features, y_samples)
    # (shape: (batch_size, num_samples))

#####
# compute loss:

```

```
#####  
f_samples = scores_samples  
p_N_samples = q_y_samples.detach()  
f_0 = scores_gt  
p_N_0 = q_ys.detach()  
exp_vals_0 = f_0-torch.log(p_N_0)  
exp_vals_samples = f_samples-torch.log(p_N_samples)  
exp_vals = torch.cat([exp_vals_0.unsqueeze(1), exp_vals_samples], dim=1)  
loss_ebm_nce = -torch.mean(exp_vals_0 - torch.logsumexp(exp_vals, dim=1))  
  
log_Z = torch.logsumexp(scores_samples.detach()  
                        - torch.log(q_y_samples), dim=1) - math.log(num_samples)  
loss_mdn_kl = torch.mean(log_Z)  
  
loss = loss_ebm_nce + loss_mdn_kl  
  
optimizer.zero_grad()  
loss.backward()  
optimizer.step()
```